Peertechz

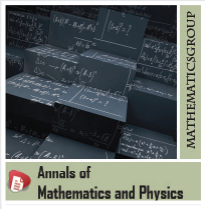

Annals of Mathematics and Physics OPEN ACCESS JOURNAL

ISSN: 2689-7636 Journal DOI: https://dx.doi.org/10.17352/amp

Mini Review

# Rayleigh's, Rician's and Gaussian's distributed Noise Modelling for MRI Data, Stability Analysis under Parameters Variation

**Ofer Aluf***

School of Electrical and Computer Engineering, Ben Gurion University of the Negev, Israel

**Submitted** : 18 April, 2026
**Accepted** : 21 May, 2026
**Published** : 22 May, 2026

***Corresponding author:** Ofer Aluf, School of Electrical and Computer Engineering, Ben Gurion University of the Negev, Israel; oferaluf@bezeqint.net

**Keywords:** Magnetic resonance (MR); Rician noise, Rician distribution, MRI, MRI magnitude images noise, Gaussian distribution, Rayleigh distribution, Rician noise, SNR, MRI linear filtering, MRI filters, non – Local Means (NLM), Anisotropic filters, PSNR, MSE, Entropy, Average execution time, SSIM, MLE, NLL, Bessel function, Heaviside step function, Rayleigh – maximum – likelihood filter algorithm, NLMeans, BM3D, VST – MCAATE, MSSIM, Hard threshold, Noise pattern, Noise free image, Delay differential equation, DDE, Characteristic equation, Time delay, Stability, Stability switching, Bifurcation, Stability analysis, Zeros, Imaginary axis, Conjugate pure imaginary roots



https://www.mathematicsgroup.us

Check for updates

## Abstract

Last Rayleigh's, Rician's, and Gaussian's distributed noise model is obtained by using negative log likelihood minimizing. In machine learning (ML), we can implement optimization by using minimization of Negative Log Likelihood (NLL). It is maximum likelihood estimation (MLE) used the minimization of Negative Log Likelihood (NLL). The summable log – probabilities come from multiplicative probabilities. The log is used to handle very small likelihoods. The negative log likelihood comes from the need to optimize objective function (cost function or loss function). It is related to Gaussian or Rayleigh or Rician probability density functions. The noise in MRI is very critical and need to be inspected deeply for dynamical behaviour. The model amplitude of a noise – free image ($I$) is delayed in time due to additional disturbances (interferences). The delay parameters influence the dynamic of the system and need to be chosen for getting stable system. The stability is inspected for best performance. The nonlinear dynamic theory gives the key criteria for stable system. Integral part of the method is to track changes in system variables over time. The system dynamical behaviour can be chaotic, counterintuitive, or unpredictable. We get the specific system parameters criteria for getting disturbances reduction.

## Introduction

In MRI Rician noise is related to image intensity in magnetic resonance (MR) amplitude images. The Rician noise has Rician distribution. The MRI magnitude images noise is evaluated from images and from correction scheme. Typically, the noise in magnitude MRI images is characterized by Gaussian distribution. We know that pure noise in magnitude is also characterized by Rayleigh distribution. The Rician noise in MRI is the thermal noise due to electrons thermal agitation. In MRI the interactions between static magnetic field and alternating current in gradient coils is the acoustic noise from magnetic resonance imaging (MRI). MRI images noise reduction can be done by convolving the noise with a smoothing function. The outcome is variance reduction in the images. It can be seen as high spatial frequencies reduction in the images. We can evaluate the MRI noises by image data signal – to – noise ratio (SNR). The noise variance is evaluated by the magneto resonance (MR) data quality. MRI image parameters are very important to the results we desire such as segmentation, noise reduction, and parameters estimation, and parameters clustering. MRI noise evaluation can be done by filtering, transform domain, and statistical evaluation. The filtering can be MRI linear filtering or non – linear filtering. The MRI linear filtering is practically done by images cleaning or enhancing. It is done by pixel values replacement with weighted sum of their neighbors, by convolution. The MRI linear works in spatial domain and frequency domain. The MRI non – linear filtering removes noise while preserving edge definition. The Non – Local Means (NLM) techniques can remove Rician noise and gets better image quality in MRI. Typically, MRI non – linear filters are



**Citation:** Aluf O. Rayleigh's, Rician's and Gaussian's distributed Noise Modelling for MRI Data, Stability Analysis under Parameters Variation. Ann Math Phys. 2026;9(3):104-116. Available from: https://dx.doi.org/10.17352/amp.000187

anisotropic filters, non-local means filters, and Bilateral filters. We need to evaluate the performances of those MRI filters. The evaluation is done by inspecting the PSNR, MSE, Entropy, average execution time, and SSIM. The statistical method is maximum likelihood (ML) estimation. Other possible statistical methods are phase error estimation, linear minimum mean square error (MSE), non-parametric estimation, and by doing analysis to function singularity. The machine learning (ML) method is also in use. MRI filtering is also can be done with discrete cosine transform based filters [1,2]. The MRI noise level estimation in background is done by Rayleigh distributed method. The key value is the MRI original signal amplitude ($I$). The magnitude image $M$, we get probability density function (PDF) equation $p(I/M)=\frac{M}{\sigma^2}e^{-[\frac{M^2+I^2}{2\sigma^2}]}H(M)J_0(\frac{IM}{\sigma^2})$.

$I$ is the amplitude of a noise – free image (original signal amplitude), $M$ is the magnitude MRI image, σ is the Gaussian noise variance, $J_0(\bullet)$ is the modified zero order Bessel function, $H(\bullet)$ is the unit step Heaviside function. The Heaviside step function $H(\bullet)$ is a discontinuous function that acts as an ON/OFF switch. It is equals to zero (0) for negative argument ($M<0$) and equals to one (1) for positive argument ($M>0$), $H(M)=\begin{cases}0 & \forall\ M<0\\ 1 & \forall\ M>0\end{cases}$. If we have image SNR very low ($\mathrm{SNR}\approx 0$) then the Rician PDF (image background) is reduced to Rayleigh distribution. If the image SNR is high enough ($\mathrm{SNR}>3\mathrm{dB}$) then the Rician distribution reduced to Gaussian distribution. The probability density function (PDF) equations for very low and high SNR values are

$$p(I/M)=\begin{cases}\frac{M}{\sigma^2}e^{-[\frac{I^2}{2\sigma^2}]}H(M) & \forall\ \mathrm{SNR}\approx 0\\ \frac{1}{\sigma^2\sqrt{2\pi}}e^{-[\frac{M^2-\sqrt{I^2+\sigma^2}}{2\sigma^2}]}H(M) & \forall\ \mathrm{SNR}>3\mathrm{dB}\end{cases} \quad (1)$$

The Rayleigh noise probability density function (PDF) is given by $f_1(x;\sigma)=\frac{x}{\sigma^2}e^{-[\frac{x^2}{2\sigma^2}]}\ \forall\ x\geq 0$ where σ is the scaling parameter and $x$ is the distributed random variable. The Rayleigh noise is non negative speckle noise. The Rayleigh noise models the two-dimension magnitude where the real and imaginary parts are independent the Gaussian noise. The Rayleigh noise average/mean value is $\sigma\sqrt{\frac{\pi}{2}}$ and the variance is equal to $(\frac{4-\pi}{2})\sigma^2$. The Rayleigh noise distribution is used in Rayleigh – maximum – likelihood filter algorithms for reducing speckled noise and preserving the edges. The Rician noise gives us the probability distributed function (PDF) of MRI pixel magnitude. We divide the Rician noise SNR values to two bands. The first band is related to low SNR values, less than two (SNR<2), where the probability distribution is skewed and "Rician bias" is happened. The "Rician bias" is a phenomenon where the image intensity increased and we get distorting of the low – intensity regions. The second Rician noise SNR values band is high band and the SNR value is beyond three (SNR > 3). Then the Rician noise distribution becomes close to Gaussian PDF, $N(A,\sigma^2)$ and the noise is similar to typical additive Gaussian noise. If the signal is equal to zero then Rician distribution is reduced to Rayleigh probability distribution. The Rician noise probability density function (PDF) is given by $p(r/v,\sigma)=\frac{r}{\sigma^2}e^{-[\frac{r^2+v^2}{2\sigma^2}]}I_0(\frac{rv}{\sigma^2})$, $r$ is the measured intensity ($r\geq 0$), ν is the signal amplitude, σ is the deviation of the Gaussian noise, and $I_0(\bullet)$ is the modified zeroth – order first kind Bessel function. In MRI images, Rician noise is a non – zero mean noise mainly in low signal regions. We use Non – Local – Means (NLMeans) algorithms for tunning Rician noise. Gaussian MRI noise is a complex Gaussian noise with zero mean and real variance, imaginary variance components. These two real and imaginary variance parts are equal in value. The Gaussian noise is linear type [3,4]. The Rician distributed noise can be approximated by Gaussian distributed noise if the Signal – to – Noise Ratios (SNR) is high enough. The Gaussian noise probability density function (PDF) for pure Gaussian noise component is $p(x)=\frac{1}{\sigma\sqrt{2\pi}}e^{-[\frac{(x-\mu)^2}{2\sigma^2}]}$, σ is the intensity of thermal noise and $x$ is the distributed random variable. The MRI images are characterized by magnitude images which are the absolute value of the complex data $M=\sqrt{[\mathrm{Re}()]^2+[\mathrm{Im}()]^2}$. The absolute value operation is nonlinear and change the noise distribution. MRI denoising methods are the way to reduce MRI noise in MRI resonance frequency $f_0$ getting better diagnostic quality and clear picture. The MRI denoising methods are filters use or using deep learning. Typically, technologies are 3D filtering (BM3D), Block matching, and non – local Means (NLM). Convolutional neural networks can be the way to achieve MRI denoising. We preserve edges and structural data information while removing noise. Typical denoising algorithm is VST – MCAATE. The peak SNR (PSNR) and similarity index measure (MSSIM) are objective image quality evolution under use. Typical denoising algorithm includes three parts, (1) stabilize noise variance, (2) decompose the image into a textures part and smooth part, (3) locally process the noise. The VST is used to convert the MRI Rician distributed noise to Gaussian noise. Then to implement sparse decomposition of image and unit which fulfil adaptive threshold function [5,6]. The threshold processing is hard threshold and the processing retain the coefficients with greater modules $\omega_{i,j}$ is the wavelet coefficient of each sub-band on $T_x$ is the adaptive threshold correspond to sub-band. $\hat{\omega}_{i,j}$ is the coefficient after threshold (Figure 1).

The main variable regarding Rayleigh's, Rician's, and Gaussian's distributed noise model is the free image amplitude noise ($I$). Brainweb simulated brain database or open science framework (OSF) is used for pre calculated Rician and Gaussian noise evaluations. The Brainweb simulated brain database provides simulated MRI data that allow to get "ground – truth" images and the amplitude noise (RF/Thermal) and intensity non – uniformity. The OSF is the open – source medical imaging datasets which includes the raw "clean" data that the simulated noisy images used in MRI. The deep learning noise – reduction models are used as noise – free reference information. The main MRI data noise is thermal or coil – based noise. It follows a complex distribution. We faced problems with filters designed for Gaussian noise which cause blurring and distortion in MRI picture. The resolution is to use Rician noise removal by Non – Local Means (NL – Means) algorithm and 3D autoencoder networks algorithm. The Rayleigh's, Rician's, and Gaussian's distributed noise model delay differential equation (DDE) taken into account the delay in time of amplitude of a noise – free image. Our conclusion is that we can get stable system for right decision of delay parameters values and other system parameters values. The nonlinear theory helps to inspect stable systems by describing the dynamic processes that give an equilibrium state after perturbation. The systems have variable complex behaviours and the stability is evaluated by using Lyapunov stability theory rather than simple linear eigenvalue. It is beyond linear approximations and use core concept such as stable system which phaced small disturbances which convert the system to unstable. It happened if disturbance is beyond specific threshold values. The types of equilibrium and stability are Lyapunov stability (perturb a system from its equilibrium and the state trajectories remain bounded within the region), asymptotic stability (the system is bounded and converges back to the exact original equilibrium point for infinity time ($t\rightarrow\infty$), and limit cycles (stable, repeating, and oscillating behaviours which do not reside at a single point).



**Citation:** Aluf O. Rayleigh's, Rician's and Gaussian's distributed Noise Modelling for MRI Data, Stability Analysis under Parameters Variation. Ann Math Phys. 2026;9(3):104-116. Available from: https://dx.doi.org/10.17352/amp.000187

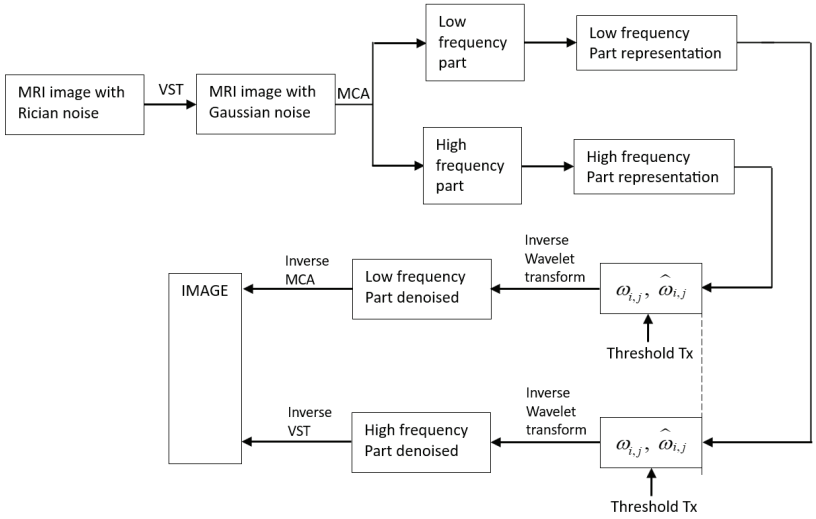


**Figure 1:** MRI denoising method flow chart

## Rayleigh's, Rician's and Gaussian's distributed Noise Model noise – free image amplitude delayed in time

The Rayleigh's, Rician's, and Gaussian's distributed noise model is characterized by differential equation with amplitude of a noise – free image ($I$) delayed in time due to additional disturbances (interferences). Under variable $I$ delayed in time ($\tau$), It becomes $I(t) \to I(t-\tau)$. We consider that the delay parameter in time does not affect the derivative in time of the amplitude of a noise – free image ($I$). We consider that the amplitude of a noise – free image ($I$) is real and positive number.

$$\frac{\partial I}{\partial t} = -[\chi_1(\frac{I(t-\tau)}{\sigma^2}) - \chi_2(\frac{2k_1}{I(t-\tau)}) + \chi_3(\frac{I(t-\tau)}{2\sigma^2\sqrt{(I^2(t-\tau)+\sigma^2)}})] + \chi.f(I(t-\tau)) \quad (2)$$

Under the transformation of amplitude of a noise – free image ($I$) partial derivative to regular derivative

$(\frac{\partial I}{\partial t} \to \frac{dI}{dt})$, we get the Rayleigh's, Rician's, and Gaussian's distributed noise model delay differential equation (DDE).

$$\frac{dI}{dt} = -[\chi_1(\frac{I(t-\tau)}{\sigma^2}) - \chi_2(\frac{2k_1}{I(t-\tau)}) + \chi_3(\frac{I(t-\tau)}{2\sigma^2\sqrt{(I^2(t-\tau)+\sigma^2)}})] + \chi.f(I(t-\tau)) \quad (3)$$

$I$ is the amplitude of a noise – free image, $I(t-\tau)$ is the amplitude of a noise – free image delayed in time, and the initial condition is $I_{t=0} = I_0$ [7]. $\sigma^2$ is the Gaussian noise variance. $X$ is the regularization parameter (constant value which balance between data attachment term and regularization function)) which achieved experimentally, $X_1$, $X_2$, and $X_3$ are the constants to be set according to noise pattern. $I_0$ is the noisy image data. $k_1$ is positive integer, $f(I)$ is the diffusion PDE based prior obtained by minimization of $E(I)$, $f(I(t-\tau))$ is the diffusion PDE as a function of amplitude of a noise – free image delayed in time. $E(I)$ is related to the minimizing process of the nonlinear energy functional ($E(I)$) of the image $I$ within $\Omega$ continuous domain by using variational outcome $E(I) = \arg\min_{\Omega}[\int_{\Omega}[L(p(I/M)) + \chi.\phi(\| \nabla I \|)]d\Omega$ where $\phi(\| \nabla I \|) = f(I)$ is the regularization function (penalty function). $L(p(I/M))$ is the negative likelihood term of Rician or Rayleigh or Gaussian distributed noise in MRI. $L(p(I/M))$ is the data attachment term (likelihood term). We get Rician, Rayleigh, and Gaussian noise removal in our system and regularization of MRI data. In $X.f(I)$ or $\chi.f(I(t-\tau))$, the $X$ indicates the start of a function $f$ which $I$ is the input parameter. We consider for simplicity that $X.f(I)$ or $\chi.f(I(t-\tau))$ are constant parameter (estimation) and equal to $\Xi$, ($\Xi = \chi.f(I(t-\tau))$). We get the Rayleigh's, Rician's, and Gaussian's distributed noise model delay differential equation:

$$\frac{dI}{dt} = -[\chi_1(\frac{I(t-\tau)}{\sigma^2}) - \chi_2(\frac{2k_1}{I(t-\tau)}) + \chi_3(\frac{I(t-\tau)}{2\sigma^2\sqrt{(I^2(t-\tau)+\sigma^2)}})] + \Xi \quad (4)$$

At fixed points (system equilibrium points) $\frac{dI}{dt} = 0$ and $\lim_{t\to\infty} I(t-\tau) \approx I(t)\ \forall\ t \gg \tau\ ;\ \tau \in \mathbb{R}\ ;\ \tau > 0$. We define amplitude of a noise – free image fixed point as $I^*$ and the system fixed points are obtained from the equation $-[\chi_1(\frac{I^*}{\sigma^2}) - \chi_2(\frac{2k_1}{I^*}) + \chi_3(\frac{I^*}{2\sigma^2\sqrt{([I^*]^2+\sigma^2)}})] + \Xi = 0$ then we get $I^*$ values and ignore negative values, complex values, and imaginary values ($I^* = \xi(\sigma, k_1, \chi_1, \chi_2, \chi_3, \Xi)$). By using Taylor series expansion

$(|I(t-\tau)| \gg \sigma^2)$, we approximate the expression $\sqrt{(I^2(t-\tau)+\sigma^2)} = |I(t-\tau)|\sqrt{1+(\frac{\sigma}{I(t-\tau)})^2}$ by $\sqrt{(I^2(t-\tau)+\sigma^2)} = |I(t-\tau)|\sqrt{1+(\frac{\sigma}{I(t-\tau)})^2} \approx |I(t-\tau)| + \frac{\sigma^2}{2|I(t-\tau)|}$. We consider that $I(t-\tau)$ is always positive then $|I(t-\tau)| = I(t-\tau)$, $\sqrt{(I^2(t-\tau)+\sigma^2)} \approx I(t-\tau) + \frac{\sigma^2}{2I(t-\tau)}$ [8]. We get the approximate Rayleigh's, Rician's, and Gaussian's distributed noise model delay differential equation (DDE):

$$\frac{dI}{dt} = -[\chi_1(\frac{I(t-\tau)}{\sigma^2}) - \chi_2(\frac{2k_1}{I(t-\tau)}) + \chi_3(\frac{I(t-\tau)}{2\sigma^2[I(t-\tau) + \frac{\sigma^2}{2I(t-\tau)}]})] + \Xi \quad (5)$$

The Rayleigh's, Rician's, and Gaussian's distributed noise model data fidelity term is derived from the noise model and paired with a regularization penalty



**Citation:** Aluf O. Rayleigh's, Rician's and Gaussian's distributed Noise Modelling for MRI Data, Stability Analysis under Parameters Variation. Ann Math Phys. 2026;9(3):104-116. Available from: https://dx.doi.org/10.17352/amp.000187

function ($\phi(\|\nabla I\|) = f(I)$). The noise model is responsible for likelihood of observed data while the regularization function is embedding prion the assumption about "true" solution. The regularization function causes to solution space restriction on by that it avoids overfitting. The penalty function is dependent on the expected structure of the signal. Types of regularization functions are $L_2$ (Ridge/Tikhonov) penalty, $L_1$ (Lasso) penalty, and Total Variation (TV), $\int|\nabla I|$ which is ideal for images which smooths noise while preserve sharp edges and boundaries. By defining the regularization function (penalty function), $\phi(\|\nabla I\|) = f(I)$ as a constant function across specific states interval we get a zero functional resistance. It causes rendering the regularization ineffective in the specific state's interval. In Rayleigh and Rician noise the regularization function penalize irregularities (noise induced spikes or bias) and vary based on the data for suppression. "Freezing" the regularization function in specific states interval helps our stability analysis.

## Rayleigh's, Rician's and Gaussian's distributed Noise Model noise – free image amplitude characteristic equation $\chi_1 = \chi_2 = 0$; $\chi_3 \neq 0$

We get the approximate Rayleigh's, Rician's, and Gaussian's distributed noise model delay differential equation (DDE) for specific noise pattern constants ($\chi_1 = \chi_2 = 0$, $\chi_3 \neq 0$).

$$\frac{dI}{dt} = -[\chi_3(\frac{I(t-\tau)}{2\sigma^2[I(t-\tau)+\frac{\sigma^2}{2I(t-\tau)}]})] + \Xi \tag{6}$$

The standard local stability analysis about the equilibrium points of Rayleigh's, Rician's, and Gaussian's distributed noise model consists in adding to coordinate $I$ (amplitude of a noise – free image) arbitrarily small increment of exponential form $ie^{\lambda t}$ and retaining the first order term $i$. The system homogeneous equation leads to a polynomial characteristics equation in the eigenvalue λ. The Rayleigh's, Rician's, and Gaussian's distributed noise model fixed values with arbitrarily small increments of exponential form $ie^{\lambda t}$ are: $k = 1$ (first fixed point), $k = 2$ (second fixed point), and $k = 3$ (third fixed point) [9].

$$I(t) = I^{(k)} + ie^{\lambda t} : I(t-\tau) = I^{(k)} + ie^{\lambda(t-\tau)} = I^{(k)} + ie^{\lambda t}e^{-\lambda\tau} \tag{7}$$

We choose the above expressions for our $I(t)$ and $I(t\text{-}\tau)$ as small displacement term $i$ from the system fixed points at time $t = 0$, $I(t) = I$, $\frac{dI}{dt} = i\lambda e^{\lambda t}$. We define $I(t) = I^{(k)} + ie^{\lambda t}\ \forall\ k \in \mathbb{N}$. Submitting $I(t)$ and $I(t\text{-}\tau)$ expressions with exponential term to Rayleigh's, Rician's, and Gaussian's distributed noise model gives $i\lambda e^{\lambda t} = -[\chi_3(\frac{I^{(k)} + ie^{\lambda t}e^{-\lambda\tau}}{2\sigma^2[I^{(k)} + ie^{\lambda t}e^{-\lambda\tau} + \frac{\sigma^2}{2(I^{(k)} + ie^{\lambda t}e^{-\lambda\tau})}]})] + \Xi$. The term $\frac{\sigma^2}{2(I^{(k)} + ie^{\lambda t}e^{-\lambda\tau})}$ is multiplied by $\frac{(I^{(k)} - ie^{\lambda t}e^{-\lambda\tau})}{(I^{(k)} - ie^{\lambda t}e^{-\lambda\tau})}$ and we get $[\frac{\sigma^2}{2(I^{(k)} + ie^{\lambda t})}][\frac{I^{(k)} - ie^{\lambda t}e^{-\lambda\tau}}{I^{(k)} - ie^{\lambda t}e^{-\lambda\tau}}] = [\frac{\sigma^2}{2}][\frac{I^{(k)} - ie^{\lambda t}e^{-\lambda\tau}}{(I^{(k)})^2 - i^2e^{2\lambda t}e^{-2\lambda\tau}}]$.

We consider $i^2 \to 0$ (very small) and we get $\frac{\sigma^2}{2(I^{(k)} + ie^{\lambda t}e^{-\lambda\tau})} \approx [\frac{\sigma^2}{2}][\frac{1}{I^{(k)}} - \frac{ie^{\lambda t}e^{-\lambda\tau}}{(I^{(k)})^2}]$.

$$I^{(k)} + ie^{\lambda t}e^{-\lambda\tau} + \frac{\sigma^2}{2(I^{(k)} + ie^{\lambda t}e^{-\lambda\tau})} = I^{(k)} + ie^{\lambda t}e^{-\lambda\tau} + [\frac{\sigma^2}{2}][\frac{1}{I^{(k)}} - \frac{ie^{\lambda t}e^{-\lambda\tau}}{(I^{(k)})^2}] \tag{8}$$

$$I^{(k)} + ie^{\lambda t}e^{-\lambda\tau} + \frac{\sigma^2}{2(I^{(k)} + ie^{\lambda t}e^{-\lambda\tau})} = I^{(k)} + \frac{\sigma^2}{2I^{(k)}} + i[1 - \frac{\sigma^2}{2(I^{(k)})^2}]e^{\lambda t}e^{-\lambda\tau} \tag{9}$$

$$\frac{I^{(k)} + ie^{\lambda t}e^{-\lambda\tau}}{2\sigma^2[I^{(k)} + ie^{\lambda t}e^{-\lambda\tau} + \frac{\sigma^2}{2(I^{(k)} + ie^{\lambda t}e^{-\lambda\tau})}]} = \frac{I^{(k)} + ie^{\lambda t}e^{-\lambda\tau}}{2\sigma^2[I^{(k)} + \frac{\sigma^2}{2I^{(k)}} + i[1 - \frac{\sigma^2}{2(I^{(k)})^2}]e^{\lambda t}e^{-\lambda\tau}]} \tag{10}$$

Multiplication above expression (10) by $\frac{(I^{(k)} + \frac{\sigma^2}{2I^{(k)}}) - i[1 - \frac{\sigma^2}{2(I^{(k)})^2}]e^{\lambda t}e^{-\lambda\tau}}{(I^{(k)} + \frac{\sigma^2}{2I^{(k)}}) - i[1 - \frac{\sigma^2}{2(I^{(k)})^2}]e^{\lambda t}e^{-\lambda\tau}}$ gives

$$\frac{I^{(k)} + ie^{\lambda t}e^{-\lambda\tau}}{2\sigma^2[I^{(k)} + ie^{\lambda t}e^{-\lambda\tau} + \frac{\sigma^2}{2(I^{(k)} + ie^{\lambda t}e^{-\lambda\tau})}]} = \frac{(I^{(k)} + ie^{\lambda t}e^{-\lambda\tau})[(I^{(k)} + \frac{\sigma^2}{2I^{(k)}}) - i[1 - \frac{\sigma^2}{2(I^{(k)})^2}]e^{\lambda t}e^{-\lambda\tau}]}{2\sigma^2[(I^{(k)} + \frac{\sigma^2}{2I^{(k)}})^2 - i^2[1 - \frac{\sigma^2}{2(I^{(k)})^2}]^2e^{2\lambda t}e^{-2\lambda\tau}]^2} \tag{11}$$

We develop the mathematical expression in the counter of the formula above (11).

$$(I^{(k)} + ie^{\lambda t}e^{-\lambda\tau})\{(I^{(k)} + \frac{\sigma^2}{2I^{(k)}}) - i[1 - \frac{\sigma^2}{2(I^{(k)})^2}]e^{\lambda t}e^{-\lambda\tau}\} = I^{(k)}(I^{(k)} + \frac{\sigma^2}{2I^{(k)}}) + i\{(I^{(k)} + \frac{\sigma^2}{2I^{(k)}}) - I^{(k)}[1 - \frac{\sigma^2}{2(I^{(k)})^2}]\}e^{\lambda t}e^{-\lambda\tau}$$
$$-i^2[1 - \frac{\sigma^2}{2(I^{(k)})^2}]e^{2\lambda t}e^{-2\lambda\tau} \tag{12}$$

We consider $i^2 \to 0$ (very small) and we get

$$(I^{(k)} + ie^{\lambda t}e^{-\lambda\tau})\{(I^{(k)} + \frac{\sigma^2}{2I^{(k)}}) - i[1 - \frac{\sigma^2}{2(I^{(k)})^2}]e^{\lambda t}e^{-\lambda\tau}\} = I^{(k)}(I^{(k)} + \frac{\sigma^2}{2I^{(k)}}) + i\{(I^{(k)} + \frac{\sigma^2}{2I^{(k)}}) - I^{(k)}[1 - \frac{\sigma^2}{2(I^{(k)})^2}]\}e^{\lambda t}e^{-\lambda\tau} \tag{13}$$

$$\frac{I^{(k)} + ie^{\lambda t}e^{-\lambda\tau}}{2\sigma^2[I^{(k)} + ie^{\lambda t}e^{-\lambda\tau} + \frac{\sigma^2}{2(I^{(k)} + ie^{\lambda t}e^{-\lambda\tau})}]} = \frac{I^{(k)}(I^{(k)} + \frac{\sigma^2}{2I^{(k)}}) + i\{(I^{(k)} + \frac{\sigma^2}{2I^{(k)}}) - I^{(k)}[1 - \frac{\sigma^2}{2(I^{(k)})^2}]\}e^{\lambda t}e^{-\lambda\tau}}{2\sigma^2[(I^{(k)} + \frac{\sigma^2}{2I^{(k)}})^2 - i^2[1 - \frac{\sigma^2}{2(I^{(k)})^2}]^2e^{2\lambda t}e^{-2\lambda\tau}]} \tag{14}$$

We consider $i^2 \to 0$ (very small) and we get

$$\frac{I^{(k)} + ie^{\lambda t}e^{-\lambda\tau}}{2\sigma^2[I^{(k)} + ie^{\lambda t}e^{-\lambda\tau} + \frac{\sigma^2}{2(I^{(k)} + ie^{\lambda t}e^{-\lambda\tau})}]} = \frac{I^{(k)}(I^{(k)} + \frac{\sigma^2}{2I^{(k)}}) + i\{(I^{(k)} + \frac{\sigma^2}{2I^{(k)}}) - I^{(k)}[1 - \frac{\sigma^2}{2(I^{(k)})^2}]\}e^{\lambda t}e^{-\lambda\tau}}{2\sigma^2(I^{(k)} + \frac{\sigma^2}{2I^{(k)}})^2} \tag{15}$$



**Citation:** Aluf O. Rayleigh's, Rician's and Gaussian's distributed Noise Modelling for MRI Data, Stability Analysis under Parameters Variation. Ann Math Phys. 2026;9(3):104-116. Available from: https://dx.doi.org/10.17352/amp.000187

$$\frac{I^{(k)}+ie^{\lambda t}e^{-\lambda\tau}}{2\sigma^2[I^{(k)}+ie^{\lambda t}e^{-\lambda\tau}+\frac{\sigma^2}{2(I^{(k)}+ie^{\lambda t}e^{-\lambda\tau})}]}=\frac{I^{(k)}}{2\sigma^2(I^{(k)}+\frac{\sigma^2}{2I^{(k)}})}+\frac{ie^{\lambda t}e^{-\lambda\tau}}{2\sigma^2(I^{(k)}+\frac{\sigma^2}{2I^{(k)}})}-i\{\frac{I^{(k)}[1-\frac{\sigma^2}{2(I^{(k)})^2}]}{2\sigma^2(I^{(k)}+\frac{\sigma^2}{2I^{(k)}})^2}\}e^{\lambda t}e^{-\lambda\tau} \tag{16}$$

$$\frac{I^{(k)}+ie^{\lambda t}e^{-\lambda\tau}}{2\sigma^2[I^{(k)}+ie^{\lambda t}e^{-\lambda\tau}+\frac{\sigma^2}{2(I^{(k)}+ie^{\lambda t}e^{-\lambda\tau})}]}=\frac{I^{(k)}}{2\sigma^2(I^{(k)}+\frac{\sigma^2}{2I^{(k)}})}+i\{\frac{1}{2\sigma^2(I^{(k)}+\frac{\sigma^2}{2I^{(k)}})}-(\frac{I^{(k)}[1-\frac{\sigma^2}{2(I^{(k)})^2}]}{2\sigma^2(I^{(k)}+\frac{\sigma^2}{2I^{(k)}})^2})\}e^{\lambda t}e^{-\lambda\tau} \tag{17}$$

The Rayleigh's, Rician's, and Gaussian's distributed noise model under $I(t)$ and $I(t\text{-}\tau)$ eigenvalue expressions submission

$i\lambda e^{\lambda t}=-[\chi_3(\frac{I^{(k)}+ie^{\lambda t}e^{-\lambda\tau}}{2\sigma^2[I^{(k)}+ie^{\lambda t}e^{-\lambda\tau}+\frac{\sigma^2}{2(I^{(k)}+ie^{\lambda t}e^{-\lambda\tau})}]})]+\Xi$ is

$$i\lambda e^{\lambda t}=-[\chi_3(\frac{I^{(k)}}{2\sigma^2(I^{(k)}+\frac{\sigma^2}{2I^{(k)}})}+i\{\frac{1}{2\sigma^2(I^{(k)}+\frac{\sigma^2}{2I^{(k)}})}-(\frac{I^{(k)}[1-\frac{\sigma^2}{2(I^{(k)})^2}]}{2\sigma^2(I^{(k)}+\frac{\sigma^2}{2I^{(k)}})^2})\}e^{\lambda t}e^{-\lambda\tau})]+\Xi \tag{18}$$

$$i\lambda e^{\lambda t}=-\chi_3(\frac{I^{(k)}}{2\sigma^2(I^{(k)}+\frac{\sigma^2}{2I^{(k)}})}+\Xi-i\chi_3\{\frac{1}{2\sigma^2(I^{(k)}+\frac{\sigma^2}{2I^{(k)}})}-(\frac{I^{(k)}[1-\frac{\sigma^2}{2(I^{(k)})^2}]}{2\sigma^2(I^{(k)}+\frac{\sigma^2}{2I^{(k)}})^2})\}e^{\lambda t}e^{-\lambda\tau} \tag{19}$$

At fixed points ($\frac{dI}{dt}=0$), (equilibrium points) $-\chi_3(\frac{I^{(k)}}{2\sigma^2(I^{(k)}+\frac{\sigma^2}{2I^{(k)}})}+\Xi=0$ then

$$\lambda=-\chi_3\{\frac{1}{2\sigma^2(I^{(k)}+\frac{\sigma^2}{2I^{(k)}})}-(\frac{I^{(k)}[1-\frac{\sigma^2}{2(I^{(k)})^2}]}{2\sigma^2(I^{(k)}+\frac{\sigma^2}{2I^{(k)}})^2})\}e^{-\lambda\tau}\ \forall\ I^{(k)}>0\ ;\ I^{(k)}\in\mathbb{R}\ ;\ k=0,1,2,... \tag{20}$$

$$\lambda+\chi_3\{\frac{1}{2\sigma^2(I^{(k)}+\frac{\sigma^2}{2I^{(k)}})}-(\frac{I^{(k)}[1-\frac{\sigma^2}{2(I^{(k)})^2}]}{2\sigma^2(I^{(k)}+\frac{\sigma^2}{2I^{(k)}})^2})\}e^{-\lambda\tau}=0\ \forall\ I^{(k)}>0\ ;\ I^{(k)}\in\mathbb{R}\ ;\ k=0,1,2,... \tag{21}$$

We define the above eigenvalue equation as general characteristic equation $D(\tau)$.

$$D(\tau)=\lambda+\chi_3\{\frac{1}{2\sigma^2(I^{(k)}+\frac{\sigma^2}{2I^{(k)}})}-(\frac{I^{(k)}[1-\frac{\sigma^2}{2(I^{(k)})^2}]}{2\sigma^2(I^{(k)}+\frac{\sigma^2}{2I^{(k)}})^2})\}e^{-\lambda\tau}\ \forall\ I^{(k)}>0\ ;\ I^{(k)}\in\mathbb{R}\ ;\ k=0,1,2,... \tag{22}$$

We study the occurrence of any possible stability switching resulting from the increase of value of the time delayτ for the general characteristics equation $D(\tau)$. Stability switching is a phenomenon in Delay Differential Equations (DDEs) where an equilibrium point alternates between being stable and unstable as a time delay parameter (τ) increases. It often triggers complex behaviours like limit cycles, quasi-periodic oscillations, or chaos. A system that is stable at (τ = 0) may lose stability when (τ) reaches a critical value. As (τ) continues to increase, the roots may cross back into the left half of the complex plane, allowing the system to regain stability, and so on.

$$D(\lambda,\tau)=P_n(\lambda,\tau)+Q_m(\lambda,\tau)e^{-\lambda\tau} \tag{23}$$

The expression for $P_n(\lambda,\tau)$: $P_n(\lambda,\tau)=\sum_{k=0}^{n}\lambda^k p_k(\tau)$ and the expression for $Q_m(\lambda,\tau)$: $Q_m(\lambda,\tau)=\sum_{k=0}^{m}\lambda^k q_k(\tau)$.

$$D(\lambda,\tau)=P_n(\lambda,\tau)+Q_m(\lambda,\tau)e^{-\lambda\tau}\ ;\ n=1\ ;\ m=0\ ;\ n>m \tag{24}$$

The expression for $P_n(\lambda,\tau)$: $P_n(\lambda,\tau)=\sum_{k=0}^{1}\lambda^k p_k(\tau)$; $p_0(\tau)=0$; $p_1(\tau)=1$ and the expression for $Q_m(\lambda,\tau)$: $Q_m(\lambda,\tau)=\sum_{k=0}^{m=0}\lambda^k q_k(\tau)$; $q_0(\tau)=\chi_3\{\frac{1}{2\sigma^2(I^{(k)}+\frac{\sigma^2}{2I^{(k)}})}-(\frac{I^{(k)}[1-\frac{\sigma^2}{2(I^{(k)})^2}]}{2\sigma^2(I^{(k)}+\frac{\sigma^2}{2I^{(k)}})^2})\}$

. The homogeneous system for $I$ leads to a characteristic equation for the eigenvalue λ. (1) If $\lambda=j\omega$, $\omega\in\mathbb{R}$ then $P(j\omega)+Q(j\omega)\neq 0$, (2) $|\frac{Q(\lambda)}{P(\lambda)}|$ is bounded for $|\lambda|\to\infty$, $\mathrm{Re}\,\lambda\geq 0$. No roots bifurcation from $\infty$, (3) $F(\omega)=|P(j\omega)|^2-|Q(j\omega)|^2$ has a finite number of zeros. Indeed, this is polynomial in ω, and (4) Each positive root $\omega(q_i,q_k)$ of $F(\omega)=0$ is continuous and differentiable with respect to $q_i,q_k$.

$$P_n(\lambda=j\omega,\tau)=j\omega\ ;\ Q_m(\lambda=j\omega,\tau)=\chi_3\{\frac{1}{2\sigma^2(I^{(k)}+\frac{\sigma^2}{2I^{(k)}})}-(\frac{I^{(k)}[1-\frac{\sigma^2}{2(I^{(k)})^2}]}{2\sigma^2(I^{(k)}+\frac{\sigma^2}{2I^{(k)}})^2})\} \tag{25}$$

$$|P(j\omega,\tau)|^2=+\omega^2\ ;\ |Q(j\omega)|^2=\chi_3^2\{\frac{1}{2\sigma^2(I^{(k)}+\frac{\sigma^2}{2I^{(k)}})}-(\frac{I^{(k)}[1-\frac{\sigma^2}{2(I^{(k)})^2}]}{2\sigma^2(I^{(k)}+\frac{\sigma^2}{2I^{(k)}})^2})\}^2 \tag{26}$$



**Citation:** Aluf O. Rayleigh's, Rician's and Gaussian's distributed Noise Modelling for MRI Data, Stability Analysis under Parameters Variation. Ann Math Phys. 2026;9(3):104-116. Available from: https://dx.doi.org/10.17352/amp.000187

$$F(\omega) = |P(j\omega)|^2 - |Q(j\omega)|^2 = \omega^2 - \chi_3^2\{\frac{1}{2\sigma^2(I^{(k)} + \frac{\sigma^2}{2I^{(k)}})} - (\frac{I^{(k)}[1 - \frac{\sigma^2}{2(I^{(k)})^2}]}{2\sigma^2(I^{(k)} + \frac{\sigma^2}{2I^{(k)}})^2})\}^2 \quad (27)$$

We define $\Phi_0 = -\chi_3^2\{\frac{1}{2\sigma^2(I^{(k)} + \frac{\sigma^2}{2I^{(k)}})} - (\frac{I^{(k)}[1 - \frac{\sigma^2}{2(I^{(k)})^2}]}{2\sigma^2(I^{(k)} + \frac{\sigma^2}{2I^{(k)}})^2})\}^2$; $\Phi_2 = +1$ (28)

It implies $\sum_{k=0}^{1}\Phi_{2k}\omega^{2k} = 0$. Its roots are given by solving the polynomial ($\sum_{k=0}^{1}\Phi_{2k}\omega^{2k} = 0$).

$$\sin\theta(\tau) = \sin(\omega\tau) = g(\omega)\ ;\ \cos\theta(\tau) = \cos(\omega\tau) = h(\omega) \quad (29)$$

$$\sin\theta(\tau) = \frac{-P_R(j\omega,\tau)Q_I(j\omega,\tau) + P_I(j\omega,\tau)Q_R(j\omega,\tau)}{|Q(j\omega,\tau)|^2} \quad (30)$$

$$\cos\theta(\tau) = -\frac{P_R(j\omega,\tau)Q_R(j\omega,\tau) + P_I(j\omega,\tau)Q_I(j\omega,\tau)}{|Q(j\omega,\tau)|^2} \quad (31)$$

Eigenvalue λ = 0 is not a root of the characteristic equation. Furthermore, $P(\lambda)$ , $Q(\lambda)$ are analytic functions as the coefficient in $P$ and $Q$ are real. Additionally, $\overline{P(-j\omega)} = P(j\omega)$ and $\overline{Q(-j\omega)} = Q(j\omega)$ thus $\lambda = j\omega$ ; $\omega > 0$ may be an eigenvalue of the characteristic equation. The analysis consists of identifying the roots of the characteristic equation situated on the imaginary axis of the complex λ plane, by increasing the parameters σ, $\chi_3$, Re λ may, at the crossing, change its sign from (-) to (+), that is from a stable focus $E^*$ to an unstable, or vice versa. This feature may be further assessed by examining the sign of the partial derivatives with respect to σ, $\chi_3$ parameters. Upon separating into real and imaginary parts, with $P = P_R + jP_I$ ; $Q = Q_R + jQ_I$ and $P_\omega = P_{R\omega} + jP_{I\omega}$ ; $Q_\omega = Q_{R\omega} + jQ_{I\omega}$ ; $P^2 = P_R^2 + P_I^2$ [10, 11]. When $(x)$ can be any Rayleigh's, Rician's, and Gaussian's distributed noise model parameters σ, $\chi_3$ and time delay τ.

$$F_\omega = 2[(P_{R\omega}P_R + P_{I\omega}P_I) - (Q_{R\omega}Q_R + Q_{I\omega}Q_I)];\ F_x = 2[(P_{Rx}P_R + P_{Ix}P_I) - (Q_{Rx}Q_R + Q_{Ix}Q_I)];\ \omega_x = \frac{-F_x}{F_\omega} \quad (32)$$

We choose our specific parameter as time delay $x = \tau$. $P_R = 0$ ; $P_I = \omega$; $Q_I = 0$ and exists

$$Q_R = \chi_3\{\frac{1}{2\sigma^2(I^{(k)} + \frac{\sigma^2}{2I^{(k)}})} - (\frac{I^{(k)}[1 - \frac{\sigma^2}{2(I^{(k)})^2}]}{2\sigma^2(I^{(k)} + \frac{\sigma^2}{2I^{(k)}})^2})\}\ ;\ Q_R = \xi_1(\sigma, I^{(k)}, \chi_3)\ ;\ |Q|^2 = Q_R^2 \quad (33)$$

Then $\sin\theta(\tau) = \frac{\omega\xi_1(\sigma, I^{(k)}, \chi_3)}{Q_R^2} = \frac{\omega}{\xi_1(\sigma, I^{(k)}, \chi_3)}$; $\cos\theta(\tau) = 0$.

$$P_{R\omega} = 0; P_{I\omega} = 1; Q_{R\omega} = 0; Q_{I\omega} = 0; P_{R\tau} = 0\ ;\ P_{I\tau} = 0\ ;\ Q_{R\tau} = 0\ ;\ Q_{I\tau} = 0; F_\omega = 2\omega \quad (34)$$

$$F_\tau = 2[(P_{R\tau}P_R + P_{I\tau}P_I) - (Q_{R\tau}Q_R + Q_{I\tau}Q_I)] = 0 \quad (35)$$

$$V = (P_RP_{I\tau} - P_IP_{R\tau}) - (Q_RQ_{I\tau} - Q_IQ_{R\tau}) = 0 \quad (36)$$

$$U = (P_RP_{I\omega} - P_IP_{R\omega}) - (Q_RQ_{I\omega} - Q_IQ_{R\omega}) \quad (37)$$

In our Rayleigh's, Rician's, and Gaussian's distributed noise model $U = 0$.

We know that $F(\omega, \tau)$ and differentiating with respect to τ we get

$$F_\omega\frac{\partial\omega}{\partial\tau} + F_\tau = 0\ ;\ \tau \in I \Rightarrow \frac{\partial\omega}{\partial\tau} = -\frac{F_\tau}{F_\omega}.$$

$$\Lambda^{-1}(\tau) = (\frac{\partial\,\mathrm{Re}\,\lambda}{\partial\tau})_{\lambda=j\omega}\ ;\ \frac{\partial\omega}{\partial\tau} = \omega_\tau = -\frac{F_\tau}{F_\omega};\ \Lambda^{-1}(\tau) = \mathrm{Re}\{\frac{-2[U + \tau|P|^2] + jF_\omega}{F_\tau + j2[V + \omega|P|^2]}\} \quad (38)$$

$$sign\{\Lambda^{-1}(\tau)\} = sign\{F_\omega\}sign\{\tau\frac{\partial\omega}{\partial\tau} + \omega + \frac{U\frac{\partial\omega}{\partial\tau} + V}{|P|^2}\};\ sign\{F_\omega\} = sign\{\omega\};\ |P|^2 = \omega^2 \neq 0 \quad (39)$$

$$V = 0\ ;\ U = 0 \Rightarrow sign\{\Lambda^{-1}(\tau)\} = sign\{F_\omega\}sign\{\tau\frac{\partial\omega}{\partial\tau} + \omega\}\ ;\ \frac{\partial\omega}{\partial\tau} = -\frac{F_\tau}{F_\omega} = 0 \quad (40)$$

$$sign\{F_\omega\} = sign\{2\omega\} = sign\{\omega\}\ ;\ sign\{\Lambda^{-1}(\tau)\} = sign\{\omega\}sign\{\tau\frac{\partial\omega}{\partial\tau} + \omega\} \quad (41)$$

$$\frac{\partial\omega}{\partial\tau} = -\frac{F_\tau}{F_\omega} = 0 \Rightarrow sign\{\Lambda^{-1}(\tau)\} = sign\{\omega\}sign\{\omega\} \quad (42)$$

We shall presently examine the possibility of stability transitions (bifurcations) in Rayleigh's, Rician's, and Gaussian's distributed noise model ($\chi_1 = \chi_2 = 0$, $\chi_3 \neq 0$) about the equilibrium points $I^{(k)}$ where $I^{(k)} > 0$ ; $I^{(k)} \in \mathbb{R}$ ; $k = 0,1,2,\ldots$, as a result of variation of delay parameter τ. Identifying the roots of our system characteristic equation ($D(\lambda,\tau)$) situated on the imaginary axis of the complex λ- plane. The increasing the delay parameter (τ), Re λ may at the crossing, change its sign from – to +, i.e from a stable focus $E^{(*)}$ to an unstable one, or vis versa [12,13]. This feature may be further assessed by examining the sign of a partial derivatives with respect



**Citation:** Aluf O. Rayleigh's, Rician's and Gaussian's distributed Noise Modelling for MRI Data, Stability Analysis under Parameters Variation. Ann Math Phys. 2026;9(3):104-116. Available from: https://dx.doi.org/10.17352/amp.000187

to τ parameter, $\Lambda^{-1}(\tau)=(\frac{\partial \mathrm{Re}\,\lambda}{\partial \tau})_{\lambda=j\omega}$ ; $\frac{\partial \omega}{\partial \tau}=\omega_{\tau}=-\frac{F_{\tau}}{F_{\omega}}$.

$$(\Lambda^{-1}(\tau)=(\frac{\partial \mathrm{Re}\,\lambda}{\partial \tau})_{\lambda=j\omega};\chi_3,\sigma,I^{(k)}I^{(k)}>0\,;I^{(k)}\in\mathbb{R}\,;k=0,1,2,\ldots)=\text{constant} \tag{43}$$

We plot 2D function $F(\omega)$, where $\chi_3=1$ for different values of $\sigma^2$ (Gaussian noise variance) and $I^{(k)}$ (amplitude of a noise – free image fixed values), $I^{(k)}>0$ and $I^{(k)}\in\mathbb{R}\,;k=0,1,2,\ldots$. Gaussian noise variance ($\sigma^2$) determines the spread of random signal noise based on a normal distribution, with values often chosen as small. It has positive numbers (typically 0.01 to 0.5) for image denoising or higher for communication simulations. We already define amplitude of a noise – free image fixed point as $I^*(I^{(k)}\to I^*\ \forall\ I^{(k)}>0)$ where $I^{(k)}\in\mathbb{R}\,;k=0,1,2,\ldots$. and the system fixed points equation ($\chi_1=\chi_2=0$, $\chi_3=1$) is $-(\frac{I^*}{2\sigma^2\sqrt{([I^*]^2+\sigma^2)}})+\Xi=0$. We already consider for simplicity that $\chi.f(I)$ or $\chi.f(I(t-\tau))$ are constant parameter (estimation) and equal to $\Xi$, ($\Xi=\chi.f(I(t-\tau))$). In Rayleigh's, Rician's, and Gaussian's noise total variation (TV), the regularization function $f(I)=|\nabla I|=\sqrt{I_x^2+I_y^2}$ and we take the assumption for simplicity $\chi.f(I)\approx 1$ or $\chi.f(I(t-\tau))\approx 1$ ($\Xi\approx 1$). Then we two groups of system fixed point for Gaussian noise variance extremum values ($\sigma^2=0.4$ and $\sigma^2=0.49$). We ignore negative values of $I^*$ and consider only negative and real values of $I^*$. $\sigma^2\to$ Sigma2 and the related MATLAB script is

MATLAB ($\sigma^2=0.4,\sigma^2=0.49$), (Ignore negative value of I*)

```
clear

Sigma2=0.4;% Other Sigma2 value is 0.49

syms I

eq1 =-(I/(2*Sigma2*sqrt(I*I+ Sigma2)))+1==0;

S = vpasolve([eq1],[I]);

sol = S;

T = array2table(sol,'VariableNames',{'I*'})
```

T = ***I**** **(σ2 = 0.4):** 0.843274042711567821866371611848 72

***I**** **(σ2 = 0.49):** 3.447279706339097418928551299024 4

We plot two 2D functions $F(\omega,\sigma^2=0.4,I^*=0.8433)$ and $F(\omega,\sigma^2=0.49,I^*=3.4473)$, (Figure 2).

$$F(\omega,I^{(k)}\ (I^{(k)}>0\,;I^{(k)}\in\mathbb{R}\,;k=0,1,2,\ldots),\sigma,\chi_3=1)=\omega^2-\{\frac{1}{2\sigma^2(I^{(k)}+\frac{\sigma^2}{2I^{(k)}})}-(\frac{I^{(k)}[1-\frac{\sigma^2}{2(I^{(k)})^2}]}{2\sigma^2(I^{(k)}+\frac{\sigma^2}{2I^{(k)}})^2})\}^2 \tag{44}$$

We find the values $\omega_k$ ($k$ = 1,2...) that fulfil $F(\omega)$ = 0 and only for those values there can be stability switching. We ignore negative, complex, and imaginary values. The stability switching function does not depend on τ parameter. We plot 2D graphs $F(\omega)$ for different values of $\sigma^2$ and $I^{(k)}$ which is $I^*$ (fixed points), $I^{(k)}>0\,;I^{(k)}\in\mathbb{R}\,;k=0,1,2,\ldots$. We plot $F(\omega)=\varsigma(\omega)$ function and detect the sign. We check for which τ parameter values $\omega$ satisfy the equations $\sin(\omega\tau)=g(\omega)$ and $\cos(\omega\tau)=h(\omega)$, where $|Q(j\omega,\tau)|^2\neq 0$ and $(g,h)\in\mathbb{R}$. The function $F(\omega)$ is related to control theory and delay differential equations (DDEs), the function $F(\omega)$ appears

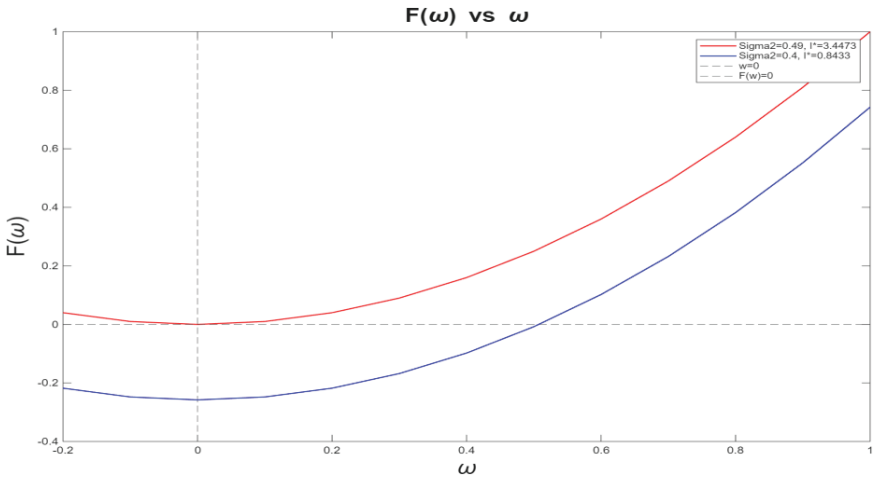


**Figure 2:** $F(\omega,I^{(k)}\ (I^{(k)}>0\,;I^{(k)}\in\mathbb{R}\,;k=0,1,2,\ldots),\sigma,\chi_1=\chi_2=0,\chi_3=1)$ functions ($\sigma^2=0.4;\sigma^2=0.49$,)



**Citation:** Aluf O. Rayleigh's, Rician's and Gaussian's distributed Noise Modelling for MRI Data, Stability Analysis under Parameters Variation. Ann Math Phys. 2026;9(3):104-116. Available from: https://dx.doi.org/10.17352/amp.000187

in Geometric Stability Switch Criteria. It used in our case to analytically determine the critical frequencies (ω) where a system changes between stable and unstable states as a time delay parameter (τ) varies. The function $F(\omega)$ typically represents the magnitude difference between the polynomial components of the system's characteristic equation.

## Rayleigh's, Rician's and Gaussian's distributed Noise Model noise – free image amplitude characteristic equation

$\chi_1 \neq 0$, $\chi_2 \neq 0$, $\chi_3 = 0$

We get the approximate Rayleigh's, Rician's, and Gaussian's distributed noise model delay differential equation (DDE) for specific noise pattern constants ($\chi_3 = 0$).

$$\frac{dI}{dt} = -[\chi_1(\frac{I(t-\tau)}{\sigma^2}) - \chi_2(\frac{2k_1}{I(t-\tau)})] + \Xi \tag{45}$$

The standard local stability analysis about the equilibrium points of Rayleigh's, Rician's, and Gaussian's distributed noise model consists in adding to coordinate $I$ (amplitude of a noise – free image) arbitrarily small increment of exponential form $ie^{\lambda t}$ and retaining the first order term $i$. The system homogeneous equation leads to a polynomial characteristics equation in the eigenvalue λ [14]. The Rayleigh's, Rician's, and Gaussian's distributed noise model fixed values with arbitrarily small increments of exponential form $ie^{\lambda t}$ are: $k = 1$ (first fixed point), $k = 2$ (second fixed point), and $k = 3$(third fixed point).

$$I(t) = I^{(k)} + ie^{\lambda t};\ I(t-\tau) = I^{(k)} + ie^{\lambda(t-\tau)} = I^{(k)} + ie^{\lambda t}e^{-\lambda\tau} \tag{46}$$

We choose the above expressions for our $I(t)$ and $I(t-\tau)$ as small displacement term $i$ from the system fixed points at time $t = 0$, $I(t) = I$, $\frac{dI}{dt} = i\lambda e^{\lambda t}$. We define $I(t) = I^{(k)} + ie^{\lambda t}\ \forall\ k \in \mathbb{N}$. Submitting $I(t)$ and $I(t-\tau)$ expressions with exponential term to Rayleigh's, Rician's, and Gaussian's distributed noise model gives $i\lambda e^{\lambda t} = -[\chi_1(\frac{I^{(k)} + ie^{\lambda t}e^{-\lambda\tau}}{\sigma^2}) - \chi_2(\frac{2k_1}{I^{(k)} + ie^{\lambda t}e^{-\lambda\tau}})] + \Xi$. The term $\frac{2k_1}{I^{(k)} + ie^{\lambda t}e^{-\lambda\tau}}$ is multiplied by $\frac{I^{(k)} - ie^{\lambda t}e^{-\lambda\tau}}{I^{(k)} - ie^{\lambda t}e^{-\lambda\tau}}$ and we get $[\frac{2k_1}{I^{(k)} + ie^{\lambda t}e^{-\lambda\tau}}][\frac{I^{(k)} - ie^{\lambda t}e^{-\lambda\tau}}{I^{(k)} - ie^{\lambda t}e^{-\lambda\tau}}] = 2k_1[\frac{I^{(k)} - ie^{\lambda t}e^{-\lambda\tau}}{(I^{(k)})^2 - i^2e^{2\lambda t}e^{-2\lambda\tau}}]$. We consider $i^2 \approx 0$ (very small) and we get $\frac{2k_1}{I^{(k)} + ie^{\lambda t}e^{-\lambda\tau}} \approx 2k_1[\frac{1}{I^{(k)}} - \frac{ie^{\lambda t}e^{-\lambda\tau}}{(I^{(k)})^2}]$.

$$i\lambda e^{\lambda t} = -\{\chi_1(\frac{I^{(k)} + ie^{\lambda t}e^{-\lambda\tau}}{\sigma^2}) - \chi_2 2k_1[\frac{1}{I^{(k)}} - \frac{ie^{\lambda t}e^{-\lambda\tau}}{(I^{(k)})^2}]\} + \Xi \tag{47}$$

$$i\lambda e^{\lambda t} = -\{\chi_1\frac{I^{(k)}}{\sigma^2} + i\chi_1\frac{e^{\lambda t}e^{-\lambda\tau}}{\sigma^2} - [\frac{\chi_2 2k_1}{I^{(k)}} - i\chi_2 2k_1\frac{e^{\lambda t}e^{-\lambda\tau}}{(I^{(k)})^2}]\} + \Xi \tag{48}$$

$$i\lambda e^{\lambda t} = -\{\chi_1\frac{I^{(k)}}{\sigma^2} - \frac{\chi_2 2k_1}{I^{(k)}}\} + \Xi - \{i[\chi_1\frac{1}{\sigma^2} + \chi_2\frac{2k_1}{(I^{(k)})^2}]e^{\lambda t}e^{-\lambda\tau}\} \tag{49}$$

At fixed points exist $-\{\chi_1\frac{I^{(k)}}{\sigma^2} - \frac{\chi_2 2k_1}{I^{(k)}}\} + \Xi = 0$ then we get the system eigenvalue equation

$$\lambda = -[\chi_1\frac{1}{\sigma^2} + \chi_2\frac{2k_1}{(I^{(k)})^2}]e^{-\lambda\tau}\ \forall\ I^{(k)} > 0;\ I^{(k)} \in \mathbb{R};\ k = 0,1,2,... \tag{50}$$

$$\lambda + [\chi_1\frac{1}{\sigma^2} + \chi_2\frac{2k_1}{(I^{(k)})^2}]e^{-\lambda\tau} = 0\ \forall\ I^{(k)} > 0;\ I^{(k)} \in \mathbb{R};\ k = 0,1,2,... \tag{51}$$

We define the above eigenvalue equation as general characteristic equation $D(\tau)$.

$$D(\lambda) = \lambda + [\chi_1\frac{1}{\sigma^2} + \chi_2\frac{2k_1}{(I^{(k)})^2}]e^{-\lambda\tau}\ \forall\ I^{(k)} > 0;\ I^{(k)} \in \mathbb{R};\ k = 0,1,2,... \tag{52}$$

We study the occurrence of any possible stability switching resulting from the increase of value of the time delay τ for the general characteristics equation $D(\tau)$.

$$D(\lambda,\tau) = P_n(\lambda,\tau) + Q_m(\lambda,\tau)e^{-\lambda\tau} \tag{53}$$

The expression for $P_n(\lambda,\tau)$: $P_n(\lambda,\tau) = \sum_{k=0}^{n}\lambda^k p_k(\tau)$ and the expression for $Q_m(\lambda,\tau)$: $Q_m(\lambda,\tau) = \sum_{k=0}^{m}\lambda^k q_k(\tau)$.

$$D(\lambda,\tau) = P_n(\lambda,\tau) + Q_m(\lambda,\tau)e^{-\lambda\tau};\ n = 1;\ m = 0;\ n > m \tag{54}$$

The expression for $P_n(\lambda,\tau)$: $P_n(\lambda,\tau) = \sum_{k=0}^{1}\lambda^k p_k(\tau)$; $p_0(\tau) = 0$; $p_1(\tau) = 1$ and the expression for $Q_m(\lambda,\tau)$: $Q_m(\lambda,\tau) = \sum_{k=0}^{m=0}\lambda^k q_k(\tau)$; $q_0(\tau) = \chi_1\frac{1}{\sigma^2} + \chi_2\frac{2k_1}{(I^{(k)})^2}$. The homogeneous system for $I$ leads to a characteristic equation for the eigenvalue λ. (1) If $\lambda = j\omega$, $\omega \in \mathbb{R}$ then $P(j\omega) + Q(j\omega) \neq 0$, (2) $|\frac{Q(\lambda)}{P(\lambda)}|$ is bounded for $|\lambda| \to \infty$, $\mathrm{Re}\,\lambda \geq 0$. No roots bifurcation from $\infty$, (3) $F(\omega) = |P(j\omega)|^2 - |Q(j\omega)|^2$ has a finite number of zeros. Indeed, this is polynomial in ω, and (4) Each positive root $\omega(q_i, q_k)$ of $F(\omega) = 0$ is continuous and differentiable with respect to $q_i$, $q_k$.

$$P_n(\lambda = j\omega,\tau) = j\omega;\ Q_m(\lambda = j\omega,\tau) = \chi_1\frac{1}{\sigma^2} + \chi_2\frac{2k_1}{(I^{(k)})^2} \tag{55}$$

$$|P(j\omega,\tau)|^2 = +\omega^2;\ |Q(j\omega)|^2 = [\chi_1\frac{1}{\sigma^2} + \chi_2\frac{2k_1}{(I^{(k)})^2}]^2 \tag{56}$$

$$F(\omega) = |P(j\omega)|^2 - |Q(j\omega)|^2 = \omega^2 - [\chi_1\frac{1}{\sigma^2} + \chi_2\frac{2k_1}{(I^{(k)})^2}]^2 \tag{57}$$

It implies $\sum_{k=0}^{1}\Phi_{2k}\omega^{2k} = 0$. Its roots are given by solving the polynomial ($\sum_{k=0}^{1}\Phi_{2k}\omega^{2k} = 0$).



**Citation:** Aluf O. Rayleigh's, Rician's and Gaussian's distributed Noise Modelling for MRI Data, Stability Analysis under Parameters Variation. Ann Math Phys. 2026;9(3):104-116. Available from: https://dx.doi.org/10.17352/amp.000187

$$\sin\theta(\tau)=\sin(\omega\tau)=g(\omega)\ ;\ \cos\theta(\tau)=\cos(\omega\tau)=h(\omega) \tag{58}$$

$$\sin\theta(\tau)=\frac{-P_R(j\omega,\tau)Q_I(j\omega,\tau)+P_I(j\omega,\tau)Q_R(j\omega,\tau)}{|Q(j\omega,\tau)|^2} \tag{59}$$

$$\cos\theta(\tau)=-\frac{P_R(j\omega,\tau)Q_R(j\omega,\tau)+P_I(j\omega,\tau)Q_I(j\omega,\tau)}{|Q(j\omega,\tau)|^2} \tag{60}$$

Eigenvalue λ = 0 is not a root of the characteristic equation. Furthermore, $P(\lambda)$, $Q(\lambda)$are analytic functions as the coefficient in $P$ and $Q$ are real. Additionally, $\overline{P(-j\omega)}=P(j\omega)$ and $\overline{Q(-j\omega)}=Q(j\omega)$ thus $\lambda=j\omega\ ;\ \omega>0$ may be an eigenvalue of the characteristic equation. The analysis consists of identifying the roots of the characteristic equation situated on the imaginary axis of the complex λ plane, by increasing the parameters σ, $\chi_1$, $\chi_2$, $\mathrm{Re}\,\lambda$ may, at the crossing, change its sign from (-) to (+), that is from a stable focus $E^*$ to an unstable, or vice versa. This feature may be further assessed by examining the sign of the partial derivatives with respect to σ, $\chi_3$ parameters. Upon separating into real and imaginary parts, with $P=P_R+jP_I\ ;\ Q=Q_R+jQ_I\ ;\ P_\omega=P_{R\omega}+jP_{I\omega}\ ;\ Q_\omega=Q_{R\omega}+jQ_{I\omega}\ ;\ P^2=P_R^2+P_I^2$. When ($x$) can be any Rayleigh's, Rician's, and Gaussian's distributed noise model parameters σ, $\chi_3$ and time delay τ [15].

$$F_\omega=2[(P_{R\omega}P_R+P_{I\omega}P_I)-(Q_{R\omega}Q_R+Q_{I\omega}Q_I)]\ ;\ F_x=2[(P_{Rx}P_R+P_{Ix}P_I)-(Q_{Rx}Q_R+Q_{Ix}Q_I)]\ ;\ \omega_x=\frac{-F_x}{F_\omega} \tag{61}$$

We choose our specific parameter as time delay $x$ = τ. $P_R=0$; $P_I=\omega$; $Q_I=0$ and exists

$$Q_R=\chi_1\frac{1}{\sigma^2}+\chi_2\frac{2k_1}{(I^{(k)})^2}\ ;\ Q_R=\xi_2(\sigma,I^{(k)},\chi_1,\chi_2)\ ;\ |Q|^2=Q_R^2 \tag{62}$$

Then $\sin\theta(\tau)=\frac{\omega\xi_2(\sigma,I^{(k)},\chi_1,\chi_2)}{Q_R^2}=\frac{\omega}{\xi_2(\sigma,I^{(k)},\chi_1,\chi_2)}\ ;\ \cos\theta(\tau)=0$

$$P_{R\omega}=0;\ P_{I\omega}=1;\ Q_{R\omega}=0;\ Q_{I\omega}=0;\ P_{R\tau}=0\ ;\ P_{I\tau}=0\ ;\ Q_{R\tau}=0\ ;\ Q_{I\tau}=0;\ F_\omega=2\omega \tag{63}$$

$$F_\tau=2[(P_{R\tau}P_R+P_{I\tau}P_I)-(\mathrm{Q}_{R\tau}Q_R+Q_{I\tau}Q_I)]=0 \tag{64}$$

$$V=(P_RP_{I\tau}-P_IP_{R\tau})-(Q_RQ_{I\tau}-Q_IQ_{R\tau})=0 \tag{65}$$

$$U=(P_RP_{I\omega}-P_IP_{R\omega})-(Q_RQ_{I\omega}-Q_IQ_{R\omega}) \tag{66}$$

In our Rayleigh's, Rician's, and Gaussian's distributed noise model $U=0$.

We know that $F(\omega,\tau)$ and differentiating with respect to τ we get

$F_\omega\frac{\partial\omega}{\partial\tau}+F_\tau=0\ ;\ \tau\in I\Rightarrow\frac{\partial\omega}{\partial\tau}=-\frac{F_\tau}{F_\omega}$.

$$\Lambda^{-1}(\tau)=(\frac{\partial\,\mathrm{Re}\,\lambda}{\partial\tau})_{\lambda=j\omega}\ ;\ \frac{\partial\omega}{\partial\tau}=\omega_\tau=-\frac{F_\tau}{F_\omega};\ \Lambda^{-1}(\tau)=\mathrm{Re}\{\frac{-2[U+\tau|P|^2]+jF_\omega}{F_\tau+j2[V+\omega|P|^2]}\} \tag{67}$$

$$sign\{\Lambda^{-1}(\tau)\}=sign\{F_\omega\}sign\{\tau\frac{\partial\omega}{\partial\tau}+\omega+\frac{U\frac{\partial\omega}{\partial\tau}+V}{|P|^2}\}\ ;\ sign\{F_\omega\}=sign\{\omega\}\ ;\ |P|^2=\omega^2\neq0 \tag{68}$$

$$V=0\ ;\ U=0\Rightarrow sign\{\Lambda^{-1}(\tau)\}=sign\{F_\omega\}sign\{\tau\frac{\partial\omega}{\partial\tau}+\omega\} \tag{69}$$

$$sign\{\Lambda^{-1}(\tau)\}=sign\{\omega\}sign\{\tau\frac{\partial\omega}{\partial\tau}+\omega\}\ ;\ \frac{\partial\omega}{\partial\tau}=-\frac{F_\tau}{F_\omega}=0 \tag{70}$$

$$\frac{\partial\omega}{\partial\tau}=-\frac{F_\tau}{F_\omega}=0\Rightarrow sign\{\Lambda^{-1}(\tau)\}=sign\{\omega\}sign\{\omega\} \tag{71}$$

We shall presently examine the possibility of stability transitions (bifurcations) in Rayleigh's, Rician's, and Gaussian's distributed noise model ($\chi_1\neq0$, $\chi_2\neq0$, $\chi_3=0$) about the equilibrium points $I^{(k)}$where $I^{(k)}>0\ ;\ I^{(k)}\in\mathbb{R}\ ;\ k=0,1,2,\ldots$, as a result of variation of delay parameter τ. Identifying the roots of our system characteristic equation ($D(\lambda,\tau)$ situated on the imaginary axis of the complex λ- plane. The increasing the delay parameter (τ), $\mathrm{Re}\,\lambda$ may at the crossing, change its sign from – to +, i.e from a stable focus $E^{(*)}$ to an unstable one, or vis versa. This feature may be further assessed by examining the sign of a partial derivatives with respect to τ parameter,

$\Lambda^{-1}(\tau)=(\frac{\partial\,\mathrm{Re}\,\lambda}{\partial\tau})_{\lambda=j\omega}\ ;\ \frac{\partial\omega}{\partial\tau}=\omega_\tau=-\frac{F_\tau}{F_\omega}$.

$$\Lambda^{-1}(\tau)=(\frac{\partial\,\mathrm{Re}\,\lambda}{\partial\tau})_{\lambda=j\omega}\ ;\ \chi_1,\ \chi_1,\ \sigma,\ I^{(k)}\ (\ I^{(k)}>0\ ;\ I^{(k)}\in\mathbb{R}\ ;\ k=0,1,2,\ldots)=\text{constant} \tag{72}$$

We plot 2D function $F(\omega)$, where $\chi_1\neq0$, $\chi_2\neq0$, $\chi_3=0$ for different values of $\sigma^2$ (Gaussian noise variance) and $I^{(k)}$(amplitude of a noise – free image fixed values), $I^{(k)}>0$and $I^{(k)}\in\mathbb{R}\ ;\ k=0,1,2,\ldots$. Gaussian noise variance ($\sigma^2$) determines the spread of random signal noise based on a normal distribution, with values often chosen as small [16]. It has positive numbers (near $F(\omega)=0$ is between 1 and 10) for image denoising or higher for communication simulations. We already define amplitude of a noise – free image fixed point as $I^*(\ I^{(k)}\to I^*\ \forall\ I^{(k)}>0\ )$ where $I^{(k)}\in\mathbb{R}\ ;\ k=0,1,2,\ldots.$ and the system fixed points equation ($\chi_1=\chi_2=1$, $\chi_3=0$) is $-\{\frac{I^{(k)}}{\sigma^2}-\frac{2k_1}{I^{(k)}}\}+\Xi=0$. We already consider for simplicity that $\chi.f(I)$ or $\chi.f(I(t-\tau))$ are constant parameter (estimation) and equal to Ξ, ($\Xi=\chi.f(I(t-\tau))$). In Rayleigh's, Rician's, and Gaussian's noise total variation (TV), the regularization function $f(I)=|\nabla I|=\sqrt{I_x^2+I_y^2}$ and we take the assumption for simplicity $\chi.f(I)\approx1$ or $\chi.f(I(t-\tau))\approx1$ ($\Xi\approx1$). $k_1$ is a positive used to calculate the Rician noise, and getting the desired output at one in the adapted method ($k_1=1$). Then we two groups of system fixed point for Gaussian noise variance extremum values ($\sigma^2=10$ and $\sigma^2=1$). $\sigma^2\to$ Sigma2 and the related MATLAB script is



**Citation:** Aluf O. Rayleigh's, Rician's and Gaussian's distributed Noise Modelling for MRI Data, Stability Analysis under Parameters Variation. Ann Math Phys. 2026;9(3):104-116. Available from: https://dx.doi.org/10.17352/amp.000187

MATLAB ($\sigma^2 = 10$ and $\sigma^2 = 1$)

```
clear
Sigma2=1;% Other Sigma2 value is 10
syms I
k1=1;
eq1 =-((I/Sigma2)-(2*k1/I))+1==0;
S = vpasolve([eq1],[I]);
sol = S;
T = array 2 table (sol,'VariableNames', {'I*'})
T =
```

**I*** ($\sigma^2 = 10$)**:** (Ignore negative value)

-1.708203932499369089227521006193 8

11.708203932499369089227521006194

**I*** ($\sigma^2 = 1$):(Ignore negative value)

——

-1.0

2.0

We plot two 2D functions $F(\omega, \sigma^2 = 10, I^* = 11.7)$ and $F(\omega, \sigma^2 = 1, I^* = 2)$, (Figure 3).

$$F(\omega, I^{(k)}\ (I^{(k)} > 0\ ;\ I^{(k)} \in \mathbb{R}\ ;\ k = 0,1,2,...), \sigma, \chi_1 = \chi_2 = 1, \chi_3 = 0, k_1 = 1) = \omega^2 - [\frac{1}{\sigma^2} + \frac{2}{(I^{(k)})^2}]^2 \quad (73)$$

We find the values $\omega_k (k = 1,2,...)$ that fulfil $F(\omega) = 0$ and only for those values there can be stability switching. We ignore negative, complex, and imaginary values. The stability switching function does not depend on $\tau$ parameter. We plot 2D graphs ($F(\omega)$) for different values of $\sigma^2$ and $I^{(k)}$ which is $I^*$ (fixed points), $I^{(k)} > 0\ ;\ I^{(k)} \in \mathbb{R}\ ;\ k = 0,1,2,....$ We plot $F(\omega) = \varsigma(\omega)$ function and detect the sign. We check for which $\tau$ parameter values $\omega$ satisfy the equations $\sin(\omega\tau) = g(\omega)$ and $\cos(\omega\tau) = h(\omega)$, where $|Q(j\omega, \tau)|^2 \neq 0$ and $(g, h) \in \mathbb{R}$ [17].

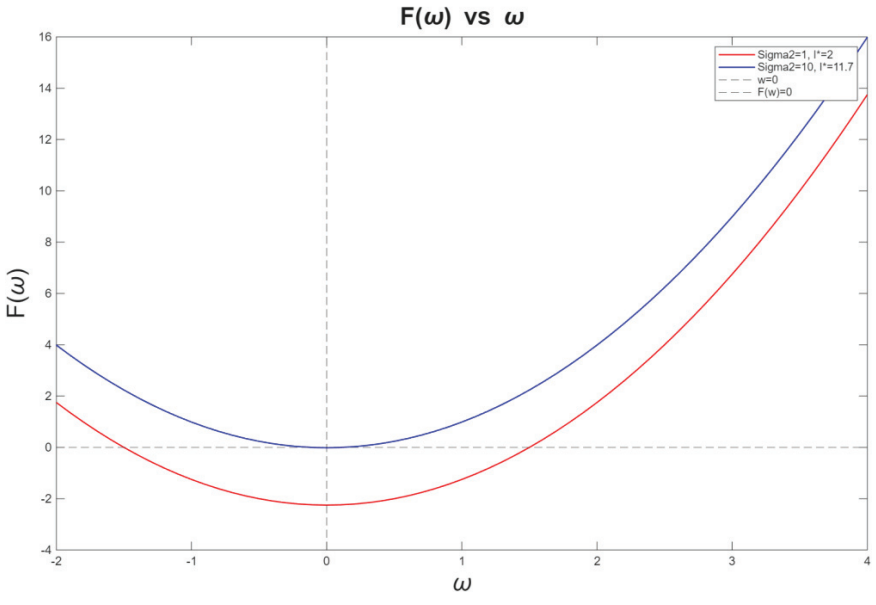


**Figure 3:** $F(\omega, I^{(k)}\ (I^{(k)} > 0\ ;\ I^{(k)} \in \mathbb{R}\ ;\ k = 0,1,2,...), \sigma, \chi_1 = \chi_2 = 1, \chi_3 = 0, k_1 = 1)$ functions $(\sigma^2 = 10, \sigma^2 = 1)$



**Citation:** Aluf O. Rayleigh's, Rician's and Gaussian's distributed Noise Modelling for MRI Data, Stability Analysis under Parameters Variation. Ann Math Phys. 2026;9(3):104-116. Available from: https://dx.doi.org/10.17352/amp.000187

## Discussion

The time delay (τ) in MRI image amplitude is basically comes from the hemodynamic response in fMRI and macroscopic blood flow transit times. The MRI system physical hardware limitations cause to time delays in MRI image amplitudes. The delay outcome is direct result from measurable phase shift and temporal dispersion between underlying event and the signal amplitude we get. In real MRI system the physical delay between the radio frequency (RF) excitation pulse and the echo peak establish the degree of transverse magnetization loss. The exact amplitude at image building is dependent on exponential relaxation times. Additionally, the ramping magnetic field gradients up and down cause to hardware heating and induced eddy currents. The eddy currents distort the magnetic field and require physical time delays in sequence timing to correct the phase errors before the sampled data. In MRI the *k* – space sampling efficiency is the key element. MRI conventional sequences fill the spatial frequency domain (k – space) sequentially. The physical limitations in gradient slew rates have effect of acquiring multi shot data which required spatial encoding delays. It influences the speed of image amplitude mapping and update.

## Conclusion

In MRI medical analysis the noise is very crucial mater. The MRI data noise influences the quality of imaging pictures. The complex additive white Gaussian noise (AWGN) can model the MRI data noise. It is especially in the raw k – space data. It follows a zero – mean Gaussian distribution (real and imaginary components). By getting magnitude images the noise becomes Rician distributed noise. It is mainly at low SNR and also at non – central chi distributed for multi – coil datasets. The statistics noise analysis is implemented in image processing applications (MRI). The noise in MRI is typically modelled by using stationary process (Rician distribution). The MRI coil is view in the concept of coil signal acquired complex Gaussian model. Magneto Resonance (MR) thermal noise is subjected to the image and the electronics noise which happened during the process of acquisition of the signal in magnet resonance (MR) receiver chain. It is related to the stochastic motion of free electrons in the MRI RF coil. It is very important in MRI to model the noise for improving the magneto resonance (MR) image quality. The MRI noise is magnitude reconstructed images is inspected for specific distribution. The MRI noise model is dependent on SNR values with the raw complex model and the final magnitude domain. The Rayleigh noise distribution is specific case of Rician distribution noise which occurs for zero signal intensity or low signal intensity compare to the noise. There are some MRI noise distributions under inspection such as Gaussian (complex raw data at any SNR), Rayleigh (background (air) at low or zero SNR), Rician (tissue foreground at low SNR (SNR < 2 dB)). The Gaussian distribution can be also for high SNR (SNR > 3) for the tissue foreground. The MRI magnitude image is the key point in subsequent transform and the Rician distribution is the key element. The original signal amplitude (*I*) gives us the probability density function (PDF) related to the magnitude image (*M*) value is $p(I / M)$. Then the Rician probability density function is reduced to Rayleigh distribution and the expression for high SNR value (SNR > 3 dB). The Rician distribution with higher SNR value becomes Gaussian distribution. The minimization process gives us the Rician Rayleigh and Gaussian noise removal and MRI data regularization. We use the maximization process of log – likelihood or minimization of the negative log – likelihood and get de – noising of image data. All of that bring us to Rayleigh's, Rician's, and Gaussian's distributed noise model which present by differential equation with amplitude of a noise – free image (*I*) as the main variable. Due to disturbances (interferences) there is variable *I* delay in time which influence the system dynamical stability. The key factors which influence the system stability and stability switching behaviour are the Gaussian noise variance ($\sigma^2$) value, amplitude of a noise – free image fixed point values $I^{(k)}$.

($I^{(k)} > 0$ ; $I^{(k)} \in \mathbb{R}$ ; $k = 0,1,2,...$), and delay parameter (τ) which related to *I* variable. Other system parameters are chosen for typical values. We get the stability dynamical behaviour for two cases, first case $\chi_1 = \chi_2 = 0$; $\chi_3 \neq 0$ and second case $\chi_1 \neq 0$, $\chi_2 \neq 0$, $\chi_3 = 0$, and plot the stability scheme. The values of Gaussian noise variance ($\sigma^2$) are chosen close to the phenomena of stability switching scenario. The outcomes and results give clear picture on system dynamic and stability behaviour [18,19].

## Appendix

### Appendix A: Lemma 1.1

Assume that $\omega(\tau)$ is a positive and real root of $F(\omega,\tau) = 0$ and is defined for $\tau \in I$, which is continuous and differentiable. Assume further that if $\lambda = j\omega$ then $P_n(j\omega,\tau) + Q_n(j\omega,\tau) \neq 0,\ \tau \in \mathbb{R}$ hold. Then the functions are continuous and differentiable on I.

### Appendix B: Theorem 1.2

Assume that $\omega(\tau)$ is a positive real root of defined for $\tau \in I,\ I \subseteq R_{+0}$, and at some $\tau^* \in I$, $S_n(\tau^*) = 0$. For some, $n \in N_0$ then a pair of simple conjugate pure imaginary roots $\lambda_+(\tau^*) = j\omega(\tau^*)$ and $\lambda_-(\tau^*) = -j\omega(\tau^*)$ of exist at $\tau = \tau^*$ which crosses the imaginary axis from left to right, $\delta(\tau^*) > 0$ and crosses the imaginary axis from right to left if then.

$$\delta(\tau^*) = sign\{\frac{d\,\mathrm{Re}\,\lambda}{d\tau}|_{\lambda=j\omega(\tau^*)}\} = sign\{F_\omega(\omega(\tau^*),\tau^*)\}sign\{\frac{dS_n(\tau)}{d\tau}|_{\tau=\tau^*}\} \quad (74)$$

The theorem becomes $sign\{\frac{d\,\mathrm{Re}\,\lambda}{d\tau}|_{\lambda=j\omega\pm}\} = sign\{\pm\Delta^{1/2}\}sign\{\frac{dS_n(\tau)}{d\tau}|_{\tau=\tau^*}\}$.

### Appendix C: Theorem 1.3

The characteristic equation $D(\lambda,\tau) = \lambda^2 + a(\tau)\lambda + b(\tau)\lambda e^{-\lambda\tau} + c(\tau) + d(\tau)e^{-\lambda\tau}$ has a pair of simple and conjugate pure imaginary roots,



Citation: Aluf O. Rayleigh's, Rician's and Gaussian's distributed Noise Modelling for MRI Data, Stability Analysis under Parameters Variation. Ann Math Phys. 2026;9(3):104-116. Available from: https://dx.doi.org/10.17352/amp.000187

real at $\tau^* \in I$ if for some $n \in N_0$. If $\omega(\tau^*) = \omega_+(\tau^*)$. This pair of simple conjugate pure imaginary roots crosses the imaginary axis from left to right if $\delta_+(\tau^*) > 0$ and crosses the imaginary axis from right to left if where $\delta_+(\tau^*)$, $\delta_+(\tau^*) = sign\{\frac{d\,\mathrm{Re}\,\lambda}{d\tau}|_{\lambda=j\omega_+(\tau^*)}\} = sign\{\frac{dS_n(\tau)}{d\tau}|_{\tau=\tau^*}\}$. If this pair of simple conjugate pure imaginary roots crosses the imaginary axis from left to right, then it crosses the imaginary axis from right to left. If where $\delta_-(\tau^*) = sign\{\frac{d\,\mathrm{Re}\,\lambda}{d\tau}|_{\lambda=j\omega_-(\tau^*)}\} = -sign\{\frac{dS_n(\tau)}{d\tau}|_{\tau=\tau^*}\}$.

If $\omega_+(\tau^*) = \omega_-(\tau^*) = \omega(\tau^*)$ then $\Delta(\tau^*) = 0$ and $sign\{\frac{d\,\mathrm{Re}\,\lambda}{d\tau}|_{\lambda=j\omega(\tau^*)}\} = 0$, the same is true when $S_n'(\tau^*) = 0$.

The following result can be useful in identifying values $\tau$ where there have been stability switches.

## Appendix D: Theorem 1.4

Assume that for all is defined as a solution of then. $\delta_\pm(\tau) = sign\{\pm\Delta^{1/2}(\tau)\}signD_\pm(\tau)$

$$D_\pm(\tau) = \omega_\pm^2[(\omega_\pm^2 b^2 + d^2) + a'(c - \omega_\pm^2) + bd' - b'd - ac'] + \omega_\pm\omega'_\pm[\tau(\omega_\pm^2 b^2 + d^2) - bd + a(c - \omega_\pm^2) + 2\omega_\pm^2 a] \quad (75)$$

$$a' = \frac{da(\tau)}{d\tau}; b' = \frac{db(\tau)}{d\tau}; c' = \frac{dc(\tau)}{d\tau}; d' = \frac{dd(\tau)}{d\tau} \quad (76)$$

## References


1. Yadav, et al. A PDE-based general framework adapted to Rayleigh's, Rician's and Gaussian's distributed noise for restoration and enhancement of MRI. J Med Phys. 2016;41(4). Available from: https://pmc.ncbi.nlm.nih.gov/articles/PMC5228049/
2. Awudong B, Yakupu P, Yan J, Li Q. Research and implementation of denoising algorithm for brain MRIs via morphological component analysis and adaptive threshold estimation. Mathematics. 2024;12(5):748. Available from: https://www.semanticscholar.org/paper/Research-and-Implementation-of-Denoising-Algorithm-Awudong-Yakupu/113121a223890d303a7a3d5bd8c398353fc0b2b6
3. Turitsyn SK, Prilepsky JE, Le ST, Wahls S, Frumin LL, Kamalian M, et al. Nonlinear Fourier transforms for optical data processing and transmission: advances and perspectives. Optica. 2017;4(3):307-322. Available from: https://opg.optica.org/optica/fulltext.cfm?uri=optica-4-3-307
4. Takata S. Linear system identification of 1-DOF vibratory system based on the maximum likelihood estimation using the analytical solution of Fokker-Planck equation. J Mech Elect Intel Syst. 2020;3(2). Available from: https://jmeis.e-jikei.org/issue/archives/0302/JMEIS030203.pdf
5. Maus M, Cotlet M, Hofkens J, Gensch T, De Schryver FC. An experimental comparison of the maximum likelihood estimation and nonlinear least-squares fluorescence lifetime analysis of single molecules. Anal Chem. 2001 May 1;73(9):2078-2086. Available from: https://doi.org/10.1021/ac000877g
6. Schoukens J, Pintelon R, Renneboog J. Maximum likelihood estimation of the parameters of linear systems. Period Polytech Electr Eng. 1989;33(4):165-182. Available from: https://pp.bme.hu/ee/article/view/4596
7. Thibault P, Guizar-Sicairos M. Maximum-likelihood refinement for coherent diffractive imaging. New J Phys. 2012;14:063004. Available from: https://iopscience.iop.org/article/10.1088/1367-2630/14/6/063004
8. Swevers J, Ganseman C, Tükel DB, De Schutter J, Van Brussel H. Optimal robot excitation and identification. IEEE Trans Robot Autom. 1997;13(5). Available from: https://scispace.com/pdf/optimal-robot-excitation-and-identification-51emb5cq0u.pdf
9. Marelli D, Fu M, Ninness B. Asymptotic optimality of the maximum-likelihood Kalman filter for Bayesian tracking with multiple nonlinear sensors. IEEE Trans Signal Process. 2015;63(17). Available from: https://www.eng.newcastle.edu.au/~mf140/home/Papers/TSP_2015_2.pdf
10. Liu Z, Wang Y, Cheng Y, Saeed T, Ye Y. Option pricing using stochastic volatility model under Fourier transform of nonlinear differential equation. Open Access Fractals. 2022;30(2):224006. Available from: https://ideas.repec.org/a/wsi/fracta/v30y2022i02ns0218348x22400655.html
11. Lin Q, Ran T, Siyong Z, Yue W. Detection and parameter estimation of multicomponent LFM signal based on the fractional Fourier transform. Sci China Ser F Inf Sci. 2004;47(2):184-198. Available from: https://www.sciengine.com/doi/10.1360/02yf0456
12. Maggio GN, Hueda MR, Agazzi OE. Maximum likelihood sequence detection receivers for nonlinear optical channels. J Electr Comput Eng. 2015;2015:736267. Available from: https://onlinelibrary.wiley.com/doi/10.1155/2015/736267
13. Soltani Bozchalooi I, Liang M. Parameter-free bearing fault detection based on maximum likelihood estimation and differentiation. Meas Sci Technol. 2009;20:065102. Available from: https://iopscience.iop.org/article/10.1088/0957-0233/20/6/065102
14. Li J, Liu X, Ren Y, Huang Z. Single-FFT receiver with pairwise maximum likelihood for layered ACO-OFDM. IEEE Photonics J. 2021;13(4). Available from: https://ieeexplore.ieee.org/stamp/stamp.jsp?arnumber=9516997




**Citation:** Aluf O. Rayleigh's, Rician's and Gaussian's distributed Noise Modelling for MRI Data, Stability Analysis under Parameters Variation. Ann Math Phys. 2026;9(3):104-116. Available from: https://dx.doi.org/10.17352/amp.000187

15. Bialkowski SE. Overcoming the multiplex disadvantage by using maximum-likelihood inversion. Appl Spectrosc. 1998;52(4). Available from: https://journals.sagepub.com/doi/10.1366/0003702981943923

16. Dai X, Zou R, An J, Li X, Sun S, Wang Y. Reducing the complexity of quasi-maximum-likelihood detectors through companding for coded MIMO systems. IEEE Trans Veh Technol. 2012;61(3). Available from: https://ui.adsabs.harvard.edu/abs/2012ITVT...61.1109D/abstract

17. Attaran B, Ghanbarzadeh A. Bearing fault detection based on maximum likelihood estimation and optimized ANN using the bees algorithm. J Appl Comput Mech. 2015;1(1):35-43. Available from: https://jacm.scu.ac.ir/article_10547_0.html

18. Gustafsson MG, Stepinski T. Studies of split spectrum processing, optimal detection, and maximum likelihood amplitude estimation using a simple clutter model. Ultrasonics. 1997;35:31-52. Available from: https://www.sciencedirect.com/science/article/pii/S0041624X96000844?__cf_chl_rt_tk=Cr4ySmmWS60n51pbjsa4Yc683i6yPHTwPA5bqQxLrz4-1779341368-1.0.1.1-ATZWQ3kZOuEVe534a0cWhNPEBwiA_md8KQwLqlmxbTY

19. Muller SP, Kijewski MF, Moore SC, Holman BL. Maximum-likelihood estimation: a mathematical model for quantitation in nuclear medicine. J Nucl Med. 1990;31(10). Available from: https://pubmed.ncbi.nlm.nih.gov/2213195/

20. Alić N, Papen GC, Saperstein RE, Milstein LB, Fainman Y. Signal statistics and maximum likelihood sequence estimation in intensity modulated fiber optic links containing a single optical preamplifier. Opt Express. 2005;13(12). Available from: https://pubmed.ncbi.nlm.nih.gov/19495371/

21. Odstrcil M, Menzel A, Guizar-Sicairos M. Iterative least-squares solver for generalized maximum-likelihood ptychography. Opt Express. 2018;26(3). Available from: https://doi.org/10.1364/oe.26.003108

22. Tong L, Perreau S. Multichannel blind identification: from subspace to maximum likelihood methods. Proc IEEE. 1998;86(10). Available from: https://acsp.ece.cornell.edu/papers/TongPerreau.pdf

23. Byrne CL, Fitzgerald RM. Spectral estimators that extend the maximum entropy and maximum likelihood methods. SIAM J Appl Math. 1984;44(2). Available from: https://epubs.siam.org/doi/10.1137/0144028

24. Fatone L, Mariani F, Recchioni MC, Zirilli F. Maximum likelihood estimation of the parameters of a system of stochastic differential equations that models the returns of the index of some classes of hedge funds. J Inverse Ill Posed Probl. 2007;15:493-526. Available from: https://www.scirp.org/reference/referencespapers?referenceid=401050

25. Akaike H. Maximum likelihood identification of Gaussian autoregressive moving average models. Biometrika. 1973;60(2):255. Available from: https://sites.stat.washington.edu/courses/stat527/s14/readings/biometrika1979.pdf

26. Kim D, Na B, Kwon SJ, Lee D, Kang W, Moon IC. Maximum likelihood training of implicit nonlinear diffusion models. In: Proceedings of the 36th Conference on Neural Information Processing Systems (NeurIPS). 2022. Available from: https://arxiv.org/abs/2205.13699

27. Strogatz SH. Nonlinear Dynamics and Chaos: With Applications to Physics, Biology, Chemistry, and Engineering. 3rd ed. Boca Raton: Chapman and Hall/CRC; 2024. Available from: https://www.biodyn.ro/course/literatura/Nonlinear_Dynamics_and_Chaos_2018_Steven_H._Strogatz.pdf

28. Beretta E, Kuang Y. Geometric stability switch criteria in delay differential systems with delay dependent parameters. SIAM J Math Anal. 2002;33(5):1144-1165. Available from: https://epubs.siam.org/doi/10.1137/S0036141000376086

29. Kuang Y. Delay Differential Equations: With Applications in Population Dynamics. San Diego: Academic Press; 2012. Available from: https://www.researchgate.net/publication/243764052_Delay_Differential_Equation_with_Application_in_Population_Dynamics

30. Gopalsamy K. *Stability and Oscillations in Delay Differential Equations of Population Dynamics.* New York (NY): Springer; 1992. Available from: https://books.google.co.in/books/about/Stability_and_Oscillations_in_Delay_Diff.html?id=BXbK_T_PSdwC&redir_esc=y




**Citation:** Aluf O. Rayleigh's, Rician's and Gaussian's distributed Noise Modelling for MRI Data, Stability Analysis under Parameters Variation. Ann Math Phys. 2026;9(3):104-116. Available from: https://dx.doi.org/10.17352/amp.000187